DIFFUSION MRI REVEALS TISSUE SPECIFIC CHANGES IN EARLY AND LATE STAGES OF DEGENERATION WITHIN THE SPINAL CORD

Torben Schneider[1], Gemma Nejati-Gilani[2,3], Mohamed Tachrount[4], Ying Li[5], Amber Hill[4], Olga Ciccarelli[4], Ken Smith[6], David Thomas[7], Daniel C Alexander[3], and Claudia A M Wheeler-Kingshott[1]

[1]NMR Research Unit, Department of Neuroinflammation, Queen Square MS Centre, UCL Institute of Neurology, London, United Kingdom, [2]Department of Infectious Disease Epidemiology, Imperial College, London, United Kingdom, [3]Centre for Medical Image Computing, Department of Computer Science, University College London, London, United Kingdom, [4]Brain Repair & Rehabilitation, UCL Institute of Neurology, London, United Kingdom, [5]Spinal Repair Unit, Brain Repair & Rehabilitation, UCL Institute of Neurology, London, United Kingdom, [6]Department of Neuroinflammation, Queen Square MS Centre, UCL Institute of Neurology, London, United Kingdom, [7]Leonard Wolfson Experimental Neurology Centre, UCL Institute of Neurology, London, United Kingdom

Target audience: Researchers interested in advanced diffusion MR models in early and late spinal cord damage.

Purpose: To test the application of an advanced diffusion MRI compartment model in early and late white matter degeneration in the spinal cord (SC), derive biomarkers of myelin and axon damage and compare with histopathological observations. Simple diffusion MRI models such as DTI[1-3] as well as more complex techniques like q-space imaging[2] (QSI) have been used previously in rodents to study the different pathological effects associated with the early and late stages of spinal cord damage. However, no attempt has been made previously to try to explicitly model the different pathological effects in the damaged white matter. Here we apply a complex compartment model of water diffusion behaviour that aims to directly reflect the intra- and extra-axonal space as well as capture diverse pathological effects associated with degeneration of myelinated axons. We apply our model in ex-vivo samples of experimental unilateral degeneration in the dorsal column and qualitatively compare our findings with histological sections within the same animals and anatomical location.

Methods *Animal model:* In 8 adult SD rats, axonal damage was inflicted by unilateral axotomy of the left L3 to L5 dorsal roots[2]. Six rats were sacrificed in the early phase of degeneration after 3 days (3d) and two more in the late phase after 30 days (30d). The rats were perfusion fixed by 4% paraformaldehyde and their spinal cord dissected. For the MRI experiment, six samples (four of 3d, two 30d) were rehydrated in phosphate-buffered saline solution 24h before scanning. The samples were then immersed in Fomblin and arranged in a custom-built sample holder. *Data acquisition:* DW images of the SCs were acquired on a 9.4T Agilent scanner using a stimulated echo (STE) imaging sequence with the following parameters: NEX=3, TE/TR=15/2800ms, FOV=25.6×12.8mm^2,matrix size=256×128, in-plane resolution 100×100µm^2, 3 slices (2mm thickness) covering the thoracic and lumbar section of the SC. The diffusion encoding parameters were: δ=2ms, Δ=15,50,100,200,300,500,750ms. For each combination of δ/Δ, DW gradients of strength G=60-600mT/m (in steps of 60mT/m) were set along 3 orthogonal directions (2 perpendicular, 1 parallel to fibre direction only for Δ=15-300ms) along with 2 unweighted images, giving a total of 194 images. *Model fitting:* We modelled the DW signal using the following compartments[4]: 1) Intra-axonal: impermeable cylinders of radius R and with diffusivity $D_{||}$; 2) Extra-axonal: cylindrically symmetric tensor with parallel diffusivity $D_{||}$ and hindered perpendicular diffusivity D_h; 3) Inflammation: isotropic tensor with diffusivity D_{iso}; 4) Stationary water[4]: isotropic restricted compartment. The relative contribution of each compartment to the measured signal is described by the four volume fractions vf_{ax}, vf_{ec}, vf_{inf}, and vf_{stat} summing up to 1. We accounted for T1 decay (due to variable Δ) and incorporated the effects of the crusher/slice select gradients[5]. The model was fit to the data using Markov chain Monte Carlo, with a burn-in of 5,000 after which 1,000 samples were collected at an interval of 20 iterations and then averaged. *Region of interest (ROI) selection:* In each sample we manually delineated the dorsal column (DC) on the non-DW image and divided it in three ROIs: left and right normal appearing white matter (NAWM) and the MRI-hyperintense site of lesion. For each sample we then calculated the mean of each model parameters per ROI. *Histology and Immunohistochemistry:* Immunostaining was carried out in one 3d and one 30d specimen. Antibody SMI-31 was used to stain for healthy axons, SMI-32 for damaged axons and Methylene blue and Azur II (LFB) for identifying the myelination.

Results and Discussion - Figure 1A summarises the means of the model parameters measured at the lesion and in both NAWM regions in the 3d and 30d injury samples. Figure 1B shows histopathology maps from one 3d and one 30d animals and the corresponding model parameter maps in the same samples at the same level of the histology. 3d samples: From histopathology we see that the loss of healthy axons (SMI31) in the early phase precedes the appearance of axonal damage (SMI32) and loss of myelin (LFB). From Figure 1, the lesion site (red outline in Figure 1B) shows the greatest difference with NAWM (little difference instead is picked up between left and right NAWM). Of the MRI parameters, lesions correspond most clearly with increased vf_{stat} and D_h. 30d-samples: At 30 days, we observe a large increase in the stationary water volume fraction, which might reflect the presence of myelin debris at the site of lesion, coinciding with an increase in SMI32 in the same region. This is further supported by the decrease of $D_{||}$ suggesting an increase in tortuosity parallel to the nerve fibres. Conversely, D_h and vf_{inf} were also higher than in NAWM, which might be explained by oedema or cell swelling. Our findings agree with previous studies of DTI[1-3] and QSI[2]. We also see an increase of apparent axon diameter along with a decrease in vf_{ax} only in the 30d lesions, while it remains largely unchanged in the 3d samples. This might indicate a specific change to the microstructure of the intra-axonal space, perhaps due to swelling or beading. Alternatively, this could be explained by increased membrane permeability or undulation[6] of the remaining axons, which would also appear as an apparent increase in the axon diameter. In contrast, R is less affected at the early phase, suggesting that this parameter is more sensitive to late-stage pathological effects. Although, R values in the 3d example in Fig 1B appear larger than in 30d, this was not replicated in the other 3d samples (Fig 1A) and might point towards a preparation artefact.

Conclusion This study demonstrated the application of a complex diffusion MRI model to early and late axonal injury. In addition to increased perpendicular diffusivity and decreased parallel diffusivity (as reported previously[1-3]) we also found that pathology manifests an increase in the amount of stationary water and a reduction in the compartment associated with axons. The mean axon diameter R was found to discriminate best between the 3d and 30d injury samples, possibly indicating additional changes to the intra-axonal microstructure and/or increased axon permeability or undulation, which change between the early and late stages of the lesion.

References: [1] Song, NI 2003 [2] Farell, MRM 2010 [3] Tu, J Neurosci&Neuroeng 2013 [4] Panagiotaki, NI 2012 [5] Lundell, NMR Biomed 2014 [6] Nilsson NMR Biomed, 2012

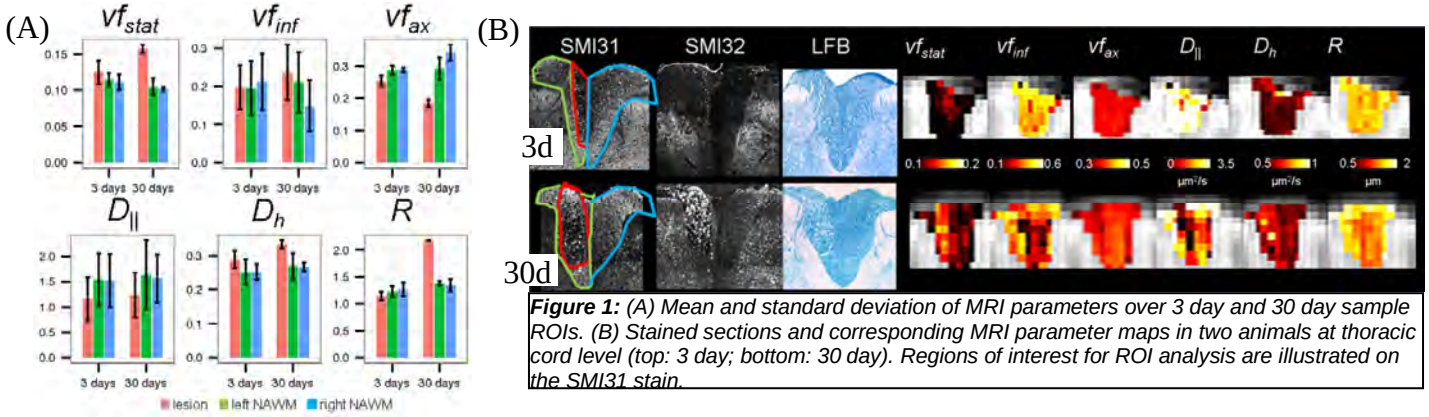

Figure 1: *(A) Mean and standard deviation of MRI parameters over 3 day and 30 day sample ROIs. (B) Stained sections and corresponding MRI parameter maps in two animals at thoracic cord level (top: 3 day; bottom: 30 day). Regions of interest for ROI analysis are illustrated on the SMI31 stain.*

We thank the UK MS Society, Department of Health's NIHR BRC, EPSRC (EP/I027084/1) and ISRT for their support.